Nicolaidou, E., Hill, T. L., & Neild, S. A. (2020). Indirect reduced-order modelling: Using nonlinear manifolds to conserve kinetic energy. *Proceedings of the Royal Society A: Mathematical, Physical and Engineering Sciences*, *476*(2243), [20200589]. https://doi.org/10.1098/rspa.2020.0589

PROCEEDINGS A

rspa.royalsocietypublishing.org

Research

Article submitted to journal

Subject Areas:
mechanical engineering,
mathematical modelling

Keywords:
reduced-order modelling, geometric nonlinearity, nonlinear normal modes, nonlinear manifold, finite element analysis, structural dynamics

Author for correspondence:
Evangelia Nicolaidou
e-mail: e.nicolaidou@bristol.ac.uk

THE ROYAL SOCIETY
PUBLISHING

Indirect reduced-order modelling: Using nonlinear manifolds to conserve kinetic energy

Evangelia Nicolaidou, Thomas L. Hill and Simon A. Neild

Department of Mechanical Engineering, University of Bristol, Bristol, BS8 1TR, UK

Nonlinear dynamic analysis of complex engineering structures modelled using commercial finite element (FE) software is computationally expensive. Indirect reduced-order modelling strategies alleviate this cost by constructing low-dimensional models using a static solution dataset from the FE model. The applicability of such methods is typically limited to structures in which (a) the main source of nonlinearity is the quasi-static coupling between transverse and in-plane modes (i.e. membrane stretching); and (b) the amount of in-plane displacement is limited. We show that the second requirement arises from the fact that, in existing methods, in-plane kinetic energy is assumed to be negligible. For structures such as thin plates and slender beams with fixed/pinned boundary conditions, this is often reasonable, but in structures with free boundary conditions (e.g. cantilever beams), this assumption is violated. Here, we exploit the concept of nonlinear manifolds to show how the in-plane kinetic energy can be accounted for in the reduced dynamics, without requiring any additional information from the FE model. This new insight enables indirect reduction methods to be applied to a far wider range of structures whilst maintaining accuracy to higher deflection amplitudes. The accuracy of the proposed method is validated using an FE model of a cantilever beam.

1. Introduction

With the ever-increasing demand for better performance, modern engineering structures continue to tend towards thin, low-weight and highly flexible designs. This trend, combined with the extreme loading environments

in which structures are often required to operate, can lead to large-amplitude vibrations, and give rise to nonlinear phenomena which have traditionally been neglected in structural dynamics. In this context, performing nonlinear dynamic analysis in an accurate and efficient manner is becoming a pressing need.

For this purpose, the Finite Element (FE) method can be used to discretise and simulate the response of continuous structures, and is standard practice in many engineering fields [1]. Whilst FE models are able to accurately capture complex geometries and directly accommodate geometric nonlinearity, the computational cost associated with the dynamic analysis of large and complex nonlinear models can be prohibitively high, particularly during optimisation procedures. In order to ease this bottleneck, reduced-order modelling methods aim to construct computationally cheap, low-dimensional models which efficiently capture the salient dynamic behaviour of the full-order FE model.

The focus of the current work is on *parametric* ROMs, in which the equations of motion (EOMs) are expressed explicitly in the form of a small set of nonlinear second-order ordinary differential equations. These can then be directly integrated in the time domain, or be used for further analytical or numerical treatment by employing any of the well-established techniques for analysing nonlinear dynamic behaviour, e.g. the harmonic balance, multiple scales or normal form methods [2–4], or numerical continuation [5,6].

In recent years, many different methods have been developed to address reduced-order modelling of geometrically nonlinear FE models. Here, we divide these methods into two broad classes: direct and indirect. In the category of *direct* methods, we include any approach which requires knowledge of the EOMs of the full-order model. For conservative, linearly elastic FE models, this typically requires access to the stiffness tensors which contain the coefficients of the quadratic and cubic monomials characterising the geometric nonlinearity [7], in addition to the linear stiffness and inertia matrices. Early works have focussed on modal reduction methods, originally developed for linear dynamics, in which the number of DOFs is reduced through a Galerkin projection onto a subset of the linear normal modes (LNMs) of the FE model [8–12]. Due to the coupling between modes, i.e. the membrane stretching induced by finite deflections/rotations in thin plates or slender beams, typically a large number of modes must be included in the reduction basis in order to accurately capture the nonlinear response. Additionally, a major drawback of such methods is that the number and type of modes needed to describe the response of the structure vary as the response amplitude increases, requiring that the reduction basis be updated during time integration [13].

These issues stem from the fact that the eigenproblem characterising the nonlinear model is configuration-dependent; the LNMs are precisely the solution of this problem at its static equilibrium, but they diverge from it as the amplitude increases. In this context, the so-called *modal derivatives* have been introduced as the second-order approximation of the state-dependent modes [14,15]. Modal derivatives can be obtained by differentiating the nonlinear eigenproblem with respect to the modal coordinates [16], thus requiring knowledge of the exact form of the nonlinearities in the EOMs[1]. Several contributions have shown that the effects of the coupling between modes can be effectively accounted for by including modal derivatives in the reduction basis, in addition to the dynamically important LNMs [18–20]. Since the number of modal derivatives grows quadratically with respect to the number of retained modes, a drawback of this approach is that the size of the reduction basis increases quickly, thus limiting the applicability of this method to relatively simple structures. To alleviate this burden, several heuristic methods for ranking and selecting the most relevant modal derivatives have been proposed [17,21]. Alternatively, the concept of a *quadratic manifold* has been proposed as a method of constraining the amplitude of the modal derivatives to that of the LNMs, rather than treating them as independent DOFs [22]. As such, reduction is achieved through a nonlinear transform consisting of a linear and a quadratic part, whose coefficients are made up of LNMs

[1]Modal derivatives can also be approximated in a non-intrusive manner using finite difference schemes and commercial FE software, however this can lead to significant numerical errors if the step width is not carefully tuned [17].

and modal derivatives, respectively. This method was found to work remarkably well for thin-walled structures characterised by von Kármán kinematics, where the quadratic enslavement of the axial modes to the bending modes is exact—however, poor results can be obtained when this assumption is not valid, as has been demonstrated using a cantilever beam [23]. This suggests that, generally, a projection onto a higher-order manifold (i.e. higher than quadratic) might be necessary to accurately capture the nonlinear behaviour of the structure.

A similar but more general concept which has been utilised for reduced-order modelling, is that of nonlinear normal modes (NNMs) defined as *invariant manifolds* in phase space [24–26]. The fundamental idea underpinning NNMs is that, through a nonlinear transform, the system can be defined in terms of a set of invariant, *normal coordinates*. In this framework, each displacement-velocity pair of normal coordinates defines an NNM, and includes the effects of all the underlying LNMs or DOFs [27]. As such, ROMs can be realised by retaining the normal coordinates associated with NNMs whose linearised natural frequencies lie in the bandwidth of interest, whilst all other coordinates can be neglected without introducing error in the process—this can be considered as the nonlinear counterpart of modal truncation methods used in linear dynamics. In its asymptotic formulation, the nonlinear transform applied to each state of the FE model, takes the form of a polynomial function spanning the reduced states [28,29]. Analytical expressions [30] for the newly introduced coefficients can be derived by substituting the transform into the full-order EOMs and equating the coefficients of like monomial terms—the dynamics of the reduced coordinates can then be expressed as a function of the coefficients of the FE model. Whilst this method provides a powerful tool for generating accurate ROMs with the fewest possible time-dependent variables, it does come with a major drawback associated with the asymptotic nature of the nonlinear projection, in addition to being intrusive. As noted in [28], the accuracy of the results can deteriorate quite rapidly in strongly nonlinear regimes, where higher orders of nonlinearity need to be considered, thus compromising the reliability of the ROM. At the same time, due to the analytical and mathematically involved nature of the method, calculations quickly become onerous when considering truncations beyond cubic.

Indirect methods are non-intrusive, i.e. they do not require knowledge of the exact full-order EOMs, and hence are applicable to models built within commercial FE software—a comprehensive review of these can be found in [31]. Such methods rely on a Galerkin projection to reduce the dimensionality of the FE model, typically onto a subset of its LNMs, such that the nonlinearities in the reduced EOMs take the form of quadratic and cubic stiffness terms which couple the retained modal coordinates. The coefficients of these nonlinear terms are approximated by extracting a set of nonlinear static solutions of the FE model, and fitting cubic polynomial functions to the static force-displacement dataset in a least-squares manner, as detailed in [32,33].

There exist two variations of indirect methods, which differ in how the static solution dataset is obtained. In the *displacement-based* approach, which is often referred to as the *enforced displacement* procedure, the structure is constrained into a prescribed shape that is a linear combination of the basis functions, and the resulting reaction forces are extracted [32,34]. The main drawback of this approach lies in the fact that, when only the low-frequency, dynamically important modes are included in the reduction basis, the ROM fails to capture the effect of membrane stretching, resulting in overly stiff behaviour [10,35]. To account for the induced in-plane motions, a number of membrane modes whose natural frequencies are well beyond the bandwidth of interest, must be explicitly included in the reduction basis [36,37]. Similarly, other strategies augment the reduction basis with the so-called *dual* or *companion* modes, which are generated using a nonlinear static or dynamic solution of the FE model, and aim to capture the membrane stretching [38–42]. As a result, not only is the identification of the relevant membrane/dual/companion modes a cumbersome procedure, but the reduction basis becomes relatively large, thus limiting the computational savings.

In the second, *force-based* variation of indirect methods, which is commonly referred to as *Implicit Condensation and Expansion* (ICE) or the *applied loads* procedure, the static solution dataset is obtained by applying a force that is a scaled superposition of the basis functions and computing

the corresponding displacement [33,43–46]. By applying a force to the structure, rather than enforcing a modal displacement, the effect of membrane stretching is captured implicitly in the nonlinear static response, thus removing the need for including any high-frequency, quasi-statically coupled modes in the reduction basis as independent DOFs. As such, the reduction basis can be constructed with only a few low-frequency transverse modes, whilst the response of the axial modes, which is assumed to be a quadratic function of the retained modal coordinates, can be reconstructed in a post-processing step [37,46]. Nevertheless, a drawback of the force-based approach is that the quality of the ROM is greatly dependent on the scaling of the forces used to obtain the training dataset. As such, scaling factors are often chosen on an ad hoc basis guided by empirical rules which predict the force necessary to exercise a "sufficient" amount of geometric nonlinearity, which often involves a trial and error process [33,37]. Recently, the authors have shown that the effect of the quasi-statically coupled axial modes can manifest in the ROM dynamics as nonlinear terms of order higher than cubic, i.e. higher than the order of nonlinearity present in the full-order model [47]. As a result, ROMs which include higher-order nonlinear terms are found to be not only more accurate, but also significantly more robust to the scaling of the training dataset, compared to their cubic counterparts. The significance of the higher-order polynomial terms in capturing quasi-static coupling in an accurate and consistent manner, reinforces the idea that linear projection frameworks are generally not well-suited to nonlinear reduced-order modelling.

Direct and indirect reduced-order modelling methods are often considered as largely distinct research areas. Methods in the former class, and specifically invariant manifold-based approaches, are supported by a rigorous mathematical framework, but due to their high analytical complexity and intrusive nature, they cannot be employed for the reduction of large-scale FE models built within commercial software. On the other hand, indirect methods are much more applicable in practice; however, their approximate nature often means that the resulting ROMs are not necessarily optimal. In this work, we aim to bridge the gap between the two classes of methods, by exploiting the concept of underlying nonlinear manifolds whilst retaining the non-intrusive nature of indirect methods. Specifically, we propose a Lagrangian approach to deriving ROMs of geometrically nonlinear structures, which aligns with the theory of NNMs defined as invariant manifolds—the proposed method may be considered as an extension to force-based indirect methods such as ICE [46]. In the standard ICE method, the projection of the static solution dataset onto the in-plane modes is used to extract a set of functions which relate the statically condensed modal displacements to the retained, transverse modal coordinates. These are only used in post-processing to recover physical deformations, stresses and strains of the FE model, but they do not influence the computed ROM. In our proposed method, the same information is utilised to enrich the ROM dynamics in order to account for the kinetic energy of the statically coupled modes, which the standard approach neglects—this additional treatment will be termed *inertial compensation*.

The rest of the paper is structured as follows. In §2, we present the theory behind force-based indirect reduction methods, and demonstrate the effectiveness and limitations of the ICE method using FE models of a clamped-clamped and a cantilever beam. In addition, we discuss how the inaccuracy of the ICE method, when considering the cantilever beam, is related to the kinetic energy of the in-plane modes. In §3, we present our proposed method of deriving nonlinear ROMs such that the kinetic energy of the statically coupled modes is retained, and in §4 we revisit the cantilever beam example to compare ROMs with and without inertial compensation. Finally, conclusions are presented in §5.

2. Applied loads method or Implicit Condensation and Expansion

(a) Theory

The equations of motion of a forced, undamped, continuous structure, discretised into N DOFs using the FE method, can be written in the form

$$\mathbf{M}\ddot{\mathbf{x}} + \mathbf{K}\mathbf{x} + \mathbf{f}_x(\mathbf{x}) = \mathbf{F}_x, \tag{2.1}$$

where $\mathbf{x}$ is the $N \times 1$ vector of generalised physical displacements, $\mathbf{M}$ and $\mathbf{K}$ are the $N \times N$ linear mass and stiffness matrices respectively, and $\mathbf{F}_x$ and $\mathbf{f}_x$ are the $N \times 1$ vectors of external and nonlinear restoring forces,[2] respectively. For reduction purposes, it is useful to consider the FE model in a space in which the coordinates are linearly uncoupled. This is achieved using the linear transform

$$\mathbf{x} = \mathbf{\Phi}\mathbf{q}, \tag{2.2}$$

where $\mathbf{\Phi}$ is the $N \times N$ matrix of mass-normalised modeshapes, such that its nth column, $\boldsymbol{\phi}_n$, solves the eigenproblem $(\mathbf{K} - \omega_n^2\mathbf{M})\boldsymbol{\phi}_n = 0$, and ω_n^2 is the corresponding eigenvalue and the square of the natural frequency of the corresponding LNM. Then, equation (2.1) is equivalent to

$$\ddot{\mathbf{q}} + \mathbf{\Lambda}\mathbf{q} + \mathbf{f}(\mathbf{q}) = \mathbf{F}, \tag{2.3}$$

where $\mathbf{q}$ is the $N \times 1$ vector of modal coordinates, $\mathbf{\Lambda}$ is the $N \times N$ diagonal eigenvalue matrix containing ω_n^2 in the nth element along its leading diagonal, and $\mathbf{f}(\mathbf{q}) = \mathbf{\Phi}^{\mathsf{T}}\mathbf{f}_x(\mathbf{\Phi}\mathbf{q})$ and $\mathbf{F} = \mathbf{\Phi}^{\mathsf{T}}\mathbf{F}_x$ are, respectively, the $N \times 1$ vectors of external and nonlinear restoring forces in the modal space. Here, we separate the LNMs of the FE model into three distinct classes: (1) a small set of dynamically important, low-frequency transverse modes, (2) a small set of high-frequency in-plane modes, which can be approximated, through geometric considerations, as being statically coupled to the transverse modes [31,46,47], and (3) the remaining modes, which are neither dynamically relevant nor statically coupled, and whose response is small enough to be neglected. Modes from each group are denoted, respectively, by the subscripts $\bullet_r$ (reduced), $\bullet_s$ (static), and $\bullet_u$ (unmodelled), such that equation (2.3) can be rewritten as

$$\begin{bmatrix} \ddot{\mathbf{q}}_r \\ \ddot{\mathbf{q}}_s \\ \ddot{\mathbf{q}}_u \end{bmatrix} + \begin{bmatrix} \mathbf{\Lambda}_r & \mathbf{0} & \mathbf{0} \\ \mathbf{0} & \mathbf{\Lambda}_s & \mathbf{0} \\ \mathbf{0} & \mathbf{0} & \mathbf{\Lambda}_u \end{bmatrix} \begin{bmatrix} \mathbf{q}_r \\ \mathbf{q}_s \\ \mathbf{q}_u \end{bmatrix} + \begin{bmatrix} \mathbf{f}_r(\mathbf{q}_r, \mathbf{q}_s, \mathbf{q}_u) \\ \mathbf{f}_s(\mathbf{q}_r, \mathbf{q}_s, \mathbf{q}_u) \\ \mathbf{f}_u(\mathbf{q}_r, \mathbf{q}_s, \mathbf{q}_u) \end{bmatrix} = \begin{bmatrix} \mathbf{F}_r \\ \mathbf{F}_s \\ \mathbf{F}_u \end{bmatrix}, \tag{2.4}$$

where the lengths of vectors $\mathbf{q}_r$, $\mathbf{q}_s$ and $\mathbf{q}_u$ are R, S and U, respectively, such that $R + S + U = N$ and $R, S \ll N$. The corresponding modeshapes are contained in matrices $\mathbf{\Phi}_r$, $\mathbf{\Phi}_s$ and $\mathbf{\Phi}_u$, whose dimensions are $N \times R$, $N \times S$ and $N \times U$, respectively.

In the ICE method [46], the dynamics of the ROM are governed only by the first group of modes, i.e. equation (2.4) is reduced to

$$\ddot{\mathbf{r}} + \mathbf{\Lambda}_r\mathbf{r} + \tilde{\mathbf{f}}_r(\mathbf{r}) = \mathbf{F}_r, \tag{2.5}$$

where $\tilde{\mathbf{f}}_r(\mathbf{r})$ is an $R \times 1$ vector of nonlinear restoring forces which must be identified using the original FE model, such that $\mathbf{r} \approx \mathbf{q}_r$. The coupling between $\mathbf{q}_s$ and $\mathbf{q}_r$ is approximated as *quasi-static*, and is here denoted by the $S \times 1$ vector function $\mathbf{g}$, i.e.

$$\mathbf{s} = \mathbf{g}(\mathbf{r}), \tag{2.6}$$

such that $\mathbf{s} \approx \mathbf{q}_s$. Physically, this may be interpreted as meaning that the displacement of the quasi-statically coupled (in-plane) modes may be determined from the displacement of the reduced (transverse) modes. Then, the physical displacement of the FE model is approximated as a

[2]It should be highlighted that, in commercial FE software, the nonlinearities are typically computed iteratively, hence the closed-form expression for $\mathbf{f}_x(\mathbf{x})$ is not accessible.

superposition of the reduced and the statically coupled modes, while the remaining modes are neglected ($\mathbf{u} = \mathbf{0} \approx \mathbf{q}_u$), i.e.

$$\mathbf{x} \approx \mathbf{\Phi}_r \mathbf{r} + \mathbf{\Phi}_s \mathbf{g}(\mathbf{r}). \tag{2.7}$$

As such, a reduction from N to R DOFs is achieved.

For the identification of $\tilde{\mathbf{f}}_r(\mathbf{r})$, it is typically assumed that the nonlinearities in the ROM take the same form as the nonlinearities in the full-order system—in the case of a linearly elastic FE model characterised by a quadratic strain-displacement relationship, each entry in $\tilde{\mathbf{f}}_r(\mathbf{r})$ then becomes a quadratic and cubic polynomial spanning the reduced modes [31]. However, as discussed in [47], to account for the effect of the statically coupled in-plane modes, the order of nonlinearity in the ROM must generally exceed that of the full-order model, such that a more robust form for $\tilde{\mathbf{f}}_r(\mathbf{r})$ is given by

$$\tilde{\mathbf{f}}_r(\mathbf{r}) = \sum_{k=2}^{K} \mathbf{A}_k \mathbf{r}^{(k)}, \tag{2.8}$$

where $\mathbf{r}^{(k)}$ is the $n_k \times 1$ vector containing all combinations of kth-order monomials involving the elements of $\mathbf{r}$, $\mathbf{A}_k$ is the $R \times n_k$ matrix containing the corresponding kth-order coefficients in each reduced equation, $K > 3$ is the truncation order, and $n_k = \dfrac{(k+R-1)!}{k!\,(R-1)!}$ is the number of kth-order terms in each reduced equation. Similarly, the quasi-static coupling functions, $\mathbf{g}(\mathbf{r})$, can be approximated as Kth-order polynomial functions[3] of the reduced modes, i.e.

$$\mathbf{g}(\mathbf{r}) = \sum_{k=2}^{K} \mathbf{B}_k \mathbf{r}^{(k)}, \tag{2.9}$$

where $\mathbf{B}_k$ is the $S \times n_k$ matrix containing the kth-order coupling coefficients for each statically coupled mode[4].

The linear properties in the reduced EOMs, (2.5), can be computed directly using the mass and stiffness matrices of the FE model; however, the coefficients in the reduced nonlinear restoring forces, $\tilde{\mathbf{f}}(\mathbf{r})$, and in the quasi-static coupling functions, $\mathbf{g}(\mathbf{r})$, are computed indirectly using a set of static solution data, as detailed in [33]. Each solution is obtained by applying a static force, $\mathbf{F}_{x0}$, that is a scaled linear combination of the reduction basis, $\mathbf{\Phi}_r$, and computing the corresponding static displacement, $\mathbf{x}_0$. The physical force to be applied is given by

$$\mathbf{F}_{x0} = \mathbf{M}\mathbf{\Phi}_r \mathbf{F}_{r0} \tag{2.10}$$

where $\mathbf{F}_{r0}$ is the $R \times 1$ vector of force scaling factors in the reduced modal space. After applying the force and extracting the resulting physical displacements, these may projected into the modal space using

$$\begin{bmatrix} \mathbf{r}_0 \\ \mathbf{s}_0 \\ \mathbf{u}_0 \end{bmatrix} = \mathbf{\Phi}^{-1} \mathbf{x}_0. \tag{2.11}$$

Finally, the coefficients in $\mathbf{A}_k$ and $\mathbf{B}_k$, for $k = \{2, \ldots, K\}$, are computed in a least-squares manner according to equations (2.8) and (2.9), using datasets of $\{\mathbf{r}_0, \mathbf{F}_{r0} - \mathbf{\Lambda}_r \mathbf{r}_0\}$ and $\{\mathbf{r}_0, \mathbf{s}_0\}$, respectively. The number of unique static solutions in the datasets must be at least equal to the number of unknown coefficients in each equation. The number of unknown coefficients in equation (2.8) can be reduced by enforcing linear dependencies between elements of $\mathbf{A}_k$ such that symmetry is preserved, and the resulting EOMs are consistent with an underlying nonlinear elastic potential energy function. This concept, which is sometimes referred to as the *constrained* ICE, as well as strategies for load case selection, are further discussed in [33].

[3] In the ICE method, a quadratic relationship is assumed.
[4] Note that $\mathbf{B}_1 = \mathbf{0}$ as $\mathbf{q}_r$ and $\mathbf{q}_s$ are linearly independent.

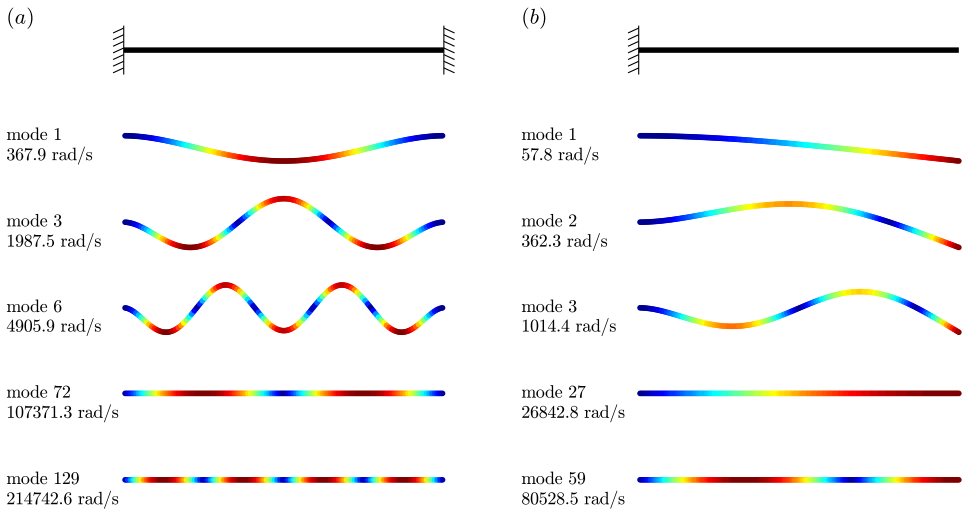

Figure 1: Modeshapes and natural frequencies of three bending and two axial LNMs of (a) the clamped-clamped beam and (b) the cantilever beam.

(b) Motivating example

In order to demonstrate the effectiveness as well as the shortcomings of the method described above, we use it to reduce two different FE models of a linearly elastic, geometrically nonlinear beam: one with clamped-clamped (C-C) and one with clamped-free (C-F) end conditions. The beams have a length, width and thickness of $\ell = 300\,\text{mm}$, $w = 25\,\text{mm}$ and $h = 1\,\text{mm}$, respectively, and are made of steel with a Young's modulus of 205 GPa, density of $7800\,\text{kg}\,\text{m}^{-3}$ and Poisson's ratio of 0.3. The models are constructed in the FE software Abaqus[5], and meshed with 120 three-node quadratic beam elements (Timoshenko type, B32), resulting in 1434 and 1440 DOFs for the C-C and the C-F beam, respectively. The shapes of the first three (symmetric) bending modes and the first two (symmetric) axial modes of the C-F (C-C) beam, as well as the corresponding natural frequencies, are shown in figure 1. The significance of these modes will be discussed later in this section.

For each FE model, we construct a single-DOF quintic ROM of the first bending mode according to equations (2.5) and (2.8) ($R = 1$, $\mathbf{r} \approx [q_1]$, $K = 5$), i.e.

$$\ddot{r}_1 + \omega_1^2 r_1 + A_2 r_1^2 + A_3 r_1^3 + A_4 r_1^4 + A_5 r_1^5 = F_1. \tag{2.12}$$

The static solution dataset used to identify the nonlinear coefficients, A_k, consists of four load cases, in which the force applied to the first mode, F_1, is equal to $\{-45, -22.5, +22.5, +45\}$. The quasi-static response of the beams for the range of applied loads is shown in figure 2, both in the physical and in the modal space[6]. The maximum vertical deflection of the tip (centre) node of the C-F (C-C) beam is $y_{\text{tip}} = 100\,\text{mm} = \ell/3$ ($y_{\text{mid}} = 1.13\,\text{mm} = 1.13h$). This corresponds to a maximum von Mises stress of 421 MPa (51.3 MPa) occurring at the clamped end(s), at which point the material approaches the limit of the linearly elastic regime.

Figure 3 shows the quasi-static coupling between the reduced mode, q_1, and the two most strongly coupled bending modes, q_2 and q_3 (q_3 and q_6), as well as the two most strongly coupled axial modes, q_{27} and q_{59} (q_{72} and q_{129}), for the C-F (C-C) beam. The modal displacement amplitudes resulting from the maximum applied static force, $F_1 = 45$, normalised with respect to the largest amplitude, are listed in table 1. It can be seen that the first mode of the C-C beam

[5]The MATLAB toolbox Abaqus2Matlab [48] was used in post-processing.

[6]Note that, in the modal space, only the response of the reduced mode and the two most strongly coupled bending and axial modes is shown.

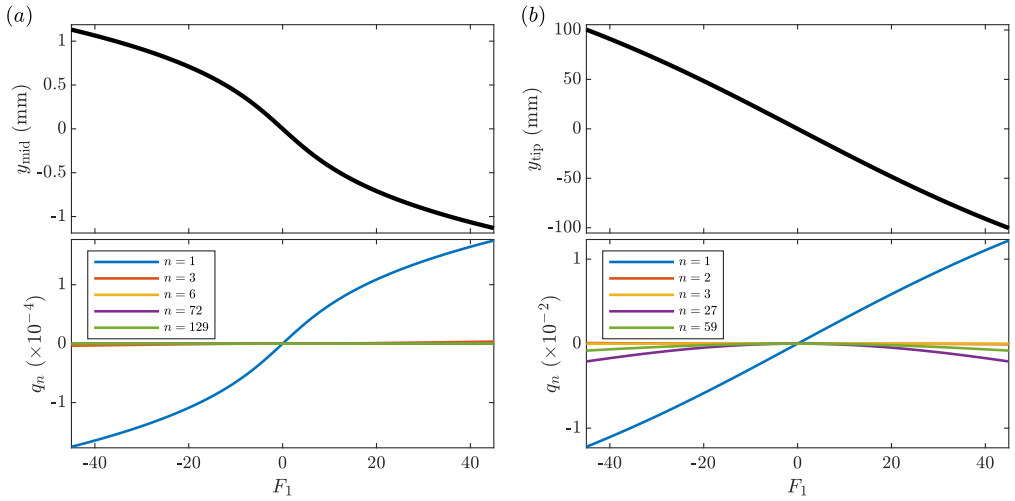

Figure 2: Quasi-static response of the beams as a function of the force applied in the first mode. The response is shown in the modal space (bottom panel) in terms of the reduced mode and the two most strongly coupled bending and axial modes, and in the physical space (top panel) in terms of the vertical displacement of (a) the centre node for the C-C beam, and (b) the tip node for the C-F beam.

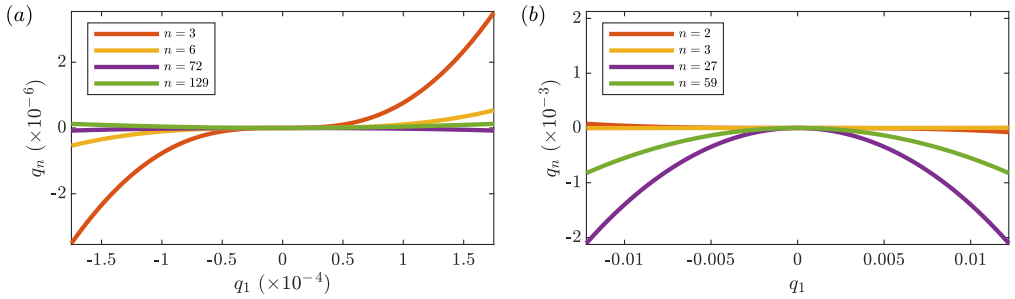

Figure 3: Static displacement of the relevant bending and axial modes as a function of the displacement in the first mode for (a) the C-C and (b) the C-F beam, when a force is applied in the first mode.

Table 1: Relative modal displacement amplitudes of the two most strongly coupled bending and axial modes, when a static force $F_1 = 45$ is applied in the first mode.

C-C	Mode no.	1	3	6	72	129
	Rel. amp.	1.0×10^{0}	2.0×10^{-2}	3.1×10^{-3}	4.5×10^{-4}	7.1×10^{-4}
C-F	Mode no.	1	2	3	27	59
	Rel. amp.	1.0×10^{0}	6.3×10^{-3}	3.8×10^{-4}	1.7×10^{-1}	6.7×10^{-2}

is most strongly coupled with third bending mode, whilst the coupling with the axial modes is less significant. Conversely, the first mode of the C-F beam exhibits weaker coupling with other bending modes, but significantly stronger coupling with axial modes—this is to be expected, as the free end of the cantilever beam allows for large in-plane displacements.

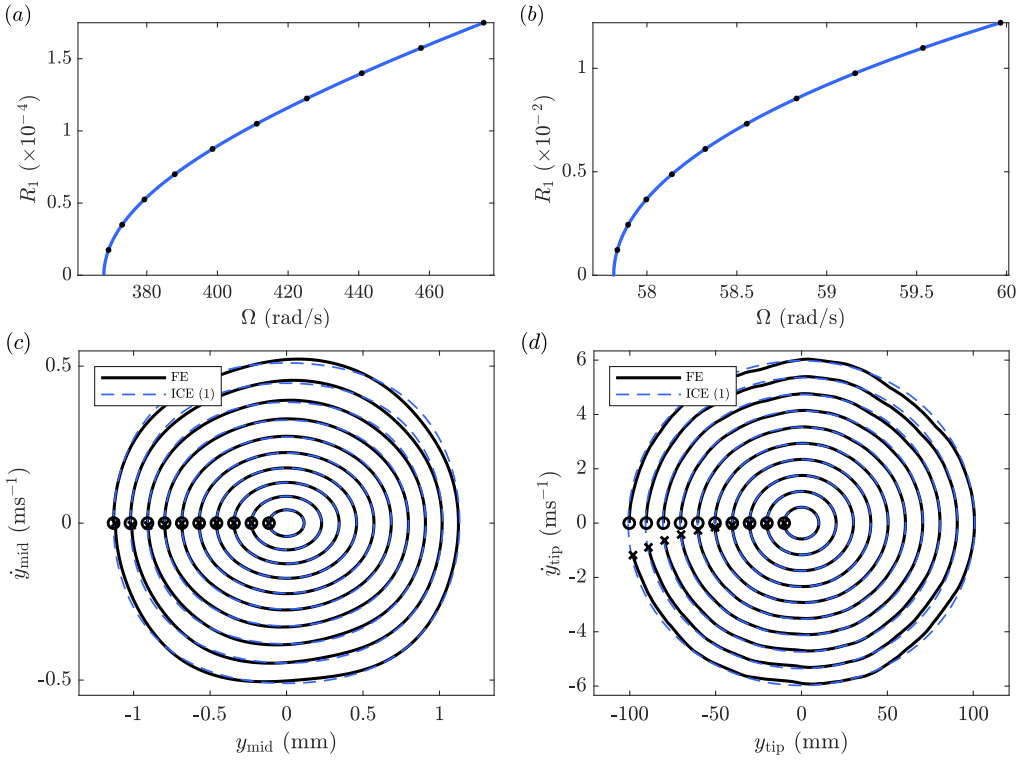

Figure 4: Top: First backbone curve of (a) the C-C and (b) the C-F beam, predicted by the quintic single-DOF ICE ROMs. These are plotted in the projection of response frequency against amplitude. Bottom: Comparison between the periodic response predicted by the ROMs (dashed lines) and the response of the FE model (solid black line), plotted in the physical phase space, for (c) the C-C and (d) the C-F beam. Ten different sets of initial conditions are considered for each ROM, and these are marked with black dots on the backbone curves. For each free response run, the FE states at time $t = 0$ and $t = T_{\Omega}$ are marked with circles and crosses, respectively.

Figure 4 (a,b) shows the backbone curves[7] of the computed single-DOF ROMs of the C-C and the C-F beams, in the projection of reduced modal amplitude, R_1, against the fundamental response frequency, Ω. Both models exhibit hardening nonlinearities due to the effect of membrane stretching induced by the large transverse displacements. It should be highlighted that the quintic ROMs presented here were found to be robust with respect to the scaling of the static solution dataset, suggesting that a higher truncation order is not necessary,[8] at least for the range of response amplitudes considered here. The accuracy of the ROMs is assessed by comparing different periodic solutions of the ROM, to the corresponding full-order free response of the FE model. To set the initial conditions of the FE model, we use the *applied modal force* method proposed in [49]. For each ROM solution, the initial modal displacement, $\mathbf{r}_0$, which occurs at zero initial velocity, is used to compute the corresponding static modal force, i.e.

$$\mathbf{F}_{r0} = \mathbf{\Lambda}_r \mathbf{r}_0 + \tilde{\mathbf{f}}_r(\mathbf{r}_0). \tag{2.13}$$

This force, projected into the physical space, is then applied to the FE model, before the structure is released from its static equilibrium at time $t = 0$ and allowed to undergo free oscillation for one

[7]Here, *backbone curves* are equivalent to NNMs defined as *families of periodic solutions* of the conservative system. These were computed using the MATLAB-based numerical continuation toolbox Continuation Core (COCO) [6].
[8]Exploring the characteristics of an FE model which might allow the required order of nonlinearity to be determined *a priori* remains a topic for future work.

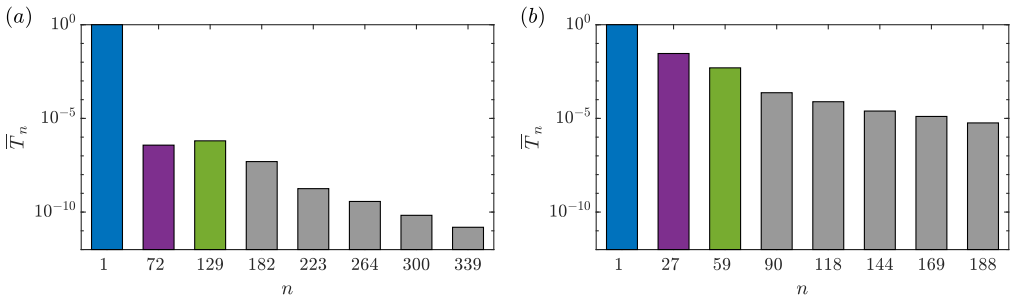

Figure 5: Normalised maximum kinetic energy in the first bending mode and the first seven axial modes, for (a) the C-C and (b) the C-F beam. These were computed from the free response of the FE model, where the initial conditions correspond to a static force of $\mathbf{F}_{r0} \approx 45$.

period of the ROM, $T_\Omega = 2\pi/\Omega$. When the state of the FE model after one ROM period coincides with its initial state, then a periodic solution is obtained and the ROM may be considered ideal. Here, we compare the initial and final state of the FE model to qualitatively assess the accuracy of each ROM.

Figure 4 (c,d) shows the FE response of the C-C and the C-F beam, respectively, obtained from ten different sets of initial conditions over one period based on the frequency predicted by the ROM (solid black line)—the FE states at $t = 0$ and $t = T_\Omega$ are marked with black circles and crosses, respectively. The corresponding periodic ROM solutions are represented by dashed blue lines. The initial reduced modal displacements used are equally spaced and marked with black dots on the backbone curves. It can be seen that the ROM of the C-C beam can very accurately predict the response frequency of the full-order NNM for the whole range of amplitudes considered here[9]. On the other hand, the ROM of the C-F beam appears to overestimate the frequency of the NNM—the period predicted by the ROM is not sufficient to allow the FE model to reach its initial state and "close" the loop in the phase space. The ROM predictions become increasingly inaccurate as the response amplitude increases. The fact that the coupling between the first and higher bending modes in the C-F beam is less significant compared to that in the C-C beam (see table 1), suggests that the inaccuracy of the C-F ROM is unlikely to stem from any unmodelled dynamic interaction with other low-frequency transverse modes. Instead, we suggest it is due to the classical observation for the cantilever beam, that there is competing action between the geometric nonlinearity, which is of the hardening type, and the in-plane inertia, which has a softening effect [50–53]. Since the ICE method is unable to capture the latter effect, it is perhaps not surprising that the resulting ROM leads to overpredictions of the response frequency.

To quantify the significance of the inertia of the statically coupled modes, we consider the kinetic energy (KE) in each mass-normalised mode, which is directly related to the resulting inertial force acting on it. We define the normalised maximum KE in each mode during a free response of the FE model, as

$$\overline{T}_n := \frac{\max\left[T_n(t)\right]}{\max\left[T_1(t)\right]} = \frac{\max\left[\dot{q}_n^2(t)\right]}{\max\left[\dot{q}_1^2(t)\right]}, \tag{2.14}$$

where T_n is the KE in the nth mode. Figure 5 shows the normalised maximum KE of the first seven axial modes of the C-C and C-F beams, for the free response with the maximum initial static force applied to the FE model. It can be seen that, for the C-C beam, the KE in the axial modes is more than six orders of magnitude smaller than that in the reduced mode. As such, the condition that in-plane inertia can be neglected, which the ICE method imposes, is a fairly good approximation.

[9]Note that for larger force scaling factors, which are not shown here, the modal interaction between the first mode and other bending modes, particularly the third one, becomes relatively more significant—in such cases, and/or when internal resonances are of interest, additional modes must be included in the reduction basis.

Conversely, the KE in the first axial modes of the C-F beam is much more significant—in this case, neglecting the effect of in-plane inertia leads to erroneous predictions. In the next section, we propose a Lagrangian-based approach for deriving nonlinear reduced-order models, such that the KE of the statically coupled modes is accounted for in the reduced dynamics.

3. Accounting for the kinetic energy of the condensed modes

(a) Proposed method

The point of departure is equation (2.4), i.e. the EOMs of the FE model, split into the reduced, statically coupled, and unmodelled, mass-normalised modal coordinates. It is assumed that Lagrangian of the system, which underpins equation (2.4), can be expressed in terms of the categorised modal coordinates as

$$\begin{aligned}\mathcal{L} &\equiv \mathcal{T}(\dot{\mathbf{q}}_r, \dot{\mathbf{q}}_s, \dot{\mathbf{q}}_u) - \mathcal{V}(\mathbf{q}_r, \mathbf{q}_s, \mathbf{q}_u) \\ &= \frac{1}{2}\left(\dot{\mathbf{q}}_r\right)^{\mathsf{T}}\dot{\mathbf{q}}_r + \frac{1}{2}\left(\dot{\mathbf{q}}_s\right)^{\mathsf{T}}\dot{\mathbf{q}}_s + \frac{1}{2}\left(\dot{\mathbf{q}}_u\right)^{\mathsf{T}}\dot{\mathbf{q}}_u - \mathcal{V}(\mathbf{q}_r, \mathbf{q}_s, \mathbf{q}_u),\end{aligned} \tag{3.1}$$

where $\mathcal{T}$ and $\mathcal{V}$ denote kinetic and potential energy functions, respectively, such that

$$\frac{\partial \mathcal{V}}{\partial \mathbf{q}_r} = \mathbf{\Lambda}_r\mathbf{q}_r + \mathbf{f}_r(\mathbf{q}_r, \mathbf{q}_s, \mathbf{q}_u), \quad \frac{\partial \mathcal{V}}{\partial \mathbf{q}_s} = \mathbf{\Lambda}_s\mathbf{q}_s + \mathbf{f}_s(\mathbf{q}_r, \mathbf{q}_s, \mathbf{q}_u), \quad \frac{\partial \mathcal{V}}{\partial \mathbf{q}_u} = \mathbf{\Lambda}_u\mathbf{q}_u + \mathbf{f}_u(\mathbf{q}_r, \mathbf{q}_s, \mathbf{q}_u). \tag{3.2}$$

Assuming that the response of the unmodelled modes ($\mathbf{q}_u$) can be neglected, the Lagrangian can be approximated as

$$\mathcal{L} \approx \hat{\mathcal{L}} = \frac{1}{2}\left(\dot{\mathbf{r}}\right)^{\mathsf{T}}\dot{\mathbf{r}} + \frac{1}{2}\left(\dot{\mathbf{s}}\right)^{\mathsf{T}}\dot{\mathbf{s}} - \hat{\mathcal{V}}(\mathbf{r}, \mathbf{s}), \tag{3.3}$$

where $\hat{\mathcal{V}}(\mathbf{r}, \mathbf{s}) := \mathcal{V}(\mathbf{r}, \mathbf{s}, \mathbf{0})$, such that $\mathbf{r} \approx \mathbf{q}_r$, $\mathbf{s} \approx \mathbf{q}_s$, $\mathbf{u} = \mathbf{0} \approx \mathbf{q}_u$, and

$$\frac{\partial \hat{\mathcal{V}}}{\partial \mathbf{r}} = \mathbf{\Lambda}_r\mathbf{r} + \hat{\mathbf{f}}_r(\mathbf{r}, \mathbf{s}), \quad \frac{\partial \hat{\mathcal{V}}}{\partial \mathbf{s}} = \mathbf{\Lambda}_s\mathbf{s} + \hat{\mathbf{f}}_s(\mathbf{r}, \mathbf{s}), \tag{3.4a}$$

$$\hat{\mathbf{f}}_r(\mathbf{r}, \mathbf{s}) := \mathbf{f}_r(\mathbf{r}, \mathbf{s}, \mathbf{0}), \quad \hat{\mathbf{f}}_s(\mathbf{r}, \mathbf{s}) := \mathbf{f}_s(\mathbf{r}, \mathbf{s}, \mathbf{0}). \tag{3.4b}$$

Using the quasi-static coupling approximation, $\mathbf{s} = \mathbf{g}(\mathbf{r})$, as given in equation (2.6), and noting that $\dot{\mathbf{s}} = \dfrac{\partial \mathbf{g}}{\partial \mathbf{r}}\dot{\mathbf{r}}$, equation (3.3) can be rewritten in terms of the reduced coordinates as

$$\hat{\mathcal{L}} = \frac{1}{2}\left(\dot{\mathbf{r}}\right)^{\mathsf{T}}\dot{\mathbf{r}} + \frac{1}{2}\left(\dot{\mathbf{r}}\right)^{\mathsf{T}}\left(\frac{\partial \mathbf{g}}{\partial \mathbf{r}}\right)^{\mathsf{T}}\frac{\partial \mathbf{g}}{\partial \mathbf{r}}\dot{\mathbf{r}} - \hat{\mathcal{V}}(\mathbf{r}, \mathbf{g}(\mathbf{r})). \tag{3.5}$$

From this, the partial derivatives of $\hat{\mathcal{L}}$ with respect to $\dot{\mathbf{r}}$ and $\mathbf{r}$, can be written, respectively, as

$$\frac{\partial \hat{\mathcal{L}}}{\partial \dot{\mathbf{r}}} = \dot{\mathbf{r}} + \left(\frac{\partial \mathbf{g}}{\partial \mathbf{r}}\right)^{\mathsf{T}}\frac{\partial \mathbf{g}}{\partial \mathbf{r}}\dot{\mathbf{r}} \tag{3.6a}$$

$$\frac{\partial \hat{\mathcal{L}}}{\partial \mathbf{r}} = \left(\frac{\partial \mathbf{g}}{\partial \mathbf{r}}\right)^{\mathsf{T}}\left(\frac{\partial^2 \mathbf{g}}{\partial \mathbf{r}^2}\dot{\mathbf{r}}\right)\dot{\mathbf{r}} - \left(\mathbf{\Lambda}_r\mathbf{r} + \hat{\mathbf{f}}_r(\mathbf{r}, \mathbf{g})\right) - \left(\frac{\partial \mathbf{g}}{\partial \mathbf{r}}\right)^{\mathsf{T}}\left(\mathbf{\Lambda}_s\mathbf{g} + \hat{\mathbf{f}}_s(\mathbf{r}, \mathbf{g})\right). \tag{3.6b}$$

According to the Euler-Lagrange equation, the reduced EOMs can be written as

$$\frac{d}{dt}\left(\frac{\partial \hat{\mathcal{L}}}{\partial \dot{\mathbf{r}}}\right) - \frac{\partial \hat{\mathcal{L}}}{\partial \mathbf{r}} = \mathbf{F}_r. \tag{3.7}$$

Substituting equations (3.6) into equation (3.7) leads to, after some algebraic manipulation,

$$\ddot{\mathbf{r}} + \left(\frac{\partial \mathbf{g}}{\partial \mathbf{r}}\right)^{\mathsf{T}}\frac{\partial \mathbf{g}}{\partial \mathbf{r}}\ddot{\mathbf{r}} + \left(\frac{\partial \mathbf{g}}{\partial \mathbf{r}}\right)^{\mathsf{T}}\left(\frac{\partial^2 \mathbf{g}}{\partial \mathbf{r}^2}\dot{\mathbf{r}}\right)\dot{\mathbf{r}} + \mathbf{\Lambda}_r\mathbf{r} + \tilde{\mathbf{f}}_r(\mathbf{r}) = \mathbf{F}_r, \tag{3.8}$$

where $\tilde{\mathbf{f}}_r(\mathbf{r}) := \hat{\mathbf{f}}_r(\mathbf{r},\mathbf{g}) + \left(\frac{\partial \mathbf{g}}{\partial \mathbf{r}}\right)^{\mathsf{T}} \left(\mathbf{\Lambda}_s \mathbf{g} + \hat{\mathbf{f}}_s(\mathbf{r},\mathbf{g})\right)$. By definition, $\mathbf{g}(\mathbf{r})$ must satisfy

$$\mathbf{\Lambda}_s \mathbf{g} + \hat{\mathbf{f}}_s(\mathbf{r},\mathbf{g}) = \mathbf{0}, \tag{3.9}$$

as it is computed based on static solution data where only the reduced modes are directly forced, while the response of the quasi-statically coupled modes is captured implicitly. As such, the second term in $\tilde{\mathbf{f}}_r(\mathbf{r})$ may be neglected, i.e. $\tilde{\mathbf{f}}_r(\mathbf{r}) = \hat{\mathbf{f}}_r(\mathbf{r},\mathbf{g})$. As with the ICE method (equation (2.5)), the reduced coordinates are related to the FE coordinates through equation (2.7), such that the number of DOFs is reduced from N to R. As with equation (2.5), equation (3.8) can be solved using numerical tools such as continuation.

(b) Indirect methods and nonlinear manifolds

The ROM obtained using our proposed method, equation (3.8), may be considered as a natural extension to the ICE ROM, equation (2.5). In both cases, the expressions for the nonlinear restoring forces, $\tilde{\mathbf{f}}_r(\mathbf{r})$, are equivalent and can be approximated, using equation (2.8), as polynomial functions in $\mathbf{r}$, whose degree must generally exceed the order of nonlinearity in the full-order model[10] [47]. However, when the kinetic energy of the in-plane modes is taken into account, two additional terms emerge in the reduced EOMs: a configuration-dependent inertia term, $\left(\frac{\partial \mathbf{g}}{\partial \mathbf{r}}\right)^{\mathsf{T}} \frac{\partial \mathbf{g}}{\partial \mathbf{r}} \ddot{\mathbf{r}}$, and a convective term, $\left(\frac{\partial \mathbf{g}}{\partial \mathbf{r}}\right)^{\mathsf{T}} \left(\frac{\partial^2 \mathbf{g}}{\partial \mathbf{r}^2} \dot{\mathbf{r}}\right) \dot{\mathbf{r}}$. The coefficients of both terms can be expressed in terms of the precomputed quasi-static coupling coefficients, $\mathbf{B}_k$, which define the relationship between the reduced and the statically coupled coordinates (equation (2.9)). As such, the proposed reduction method does not require that any additional information be extracted from the FE model—instead, the existing information is used, after some computationally cheap post-processing, to enrich the ROM dynamics. The inclusion of these additional terms in the reduced dynamics will be referred to as *inertial compensation*, and the corresponding model, i.e. equation (3.8), will be referred to as ICE-IC ROM. A schematic of the ROM generation procedure using the ICE-IC method is shown in figure 6, where the extension proposed herein is represented in red.

The importance of retaining the effect of in-plane inertia, compared to the static condensation approach, has previously been demonstrated using the concept of modal derivatives and the so-called *quadratic manifold* [22,54]. In the quadratic manifold approach, reduction is achieved through a nonlinear mapping between the FE coordinates and a small set of modal coordinates—the mapping is quadratic, and it is defined such that its gradient is given by linear modeshapes, and its curvature is given by modal derivatives. While this approach was found to provide excellent accuracy in some cases, its applicability is limited to structures characterised by von Kármán kinematics, and in which the dominant source of nonlinearity is membrane stretching [22,23]. Compared to the quadratic manifold approach, the merits of the ICE-IC method are twofold. Firstly, the relationship between the reduced and the statically coupled modes is not limited to being quadratic, which allows the method to be applied to a broader class of structures. In addition, the proposed method is non-intrusive in nature, and can be applied using any commercial FE software package. Nevertheless, the inertial compensation approach aligns with the idea underpinning nonlinear manifolds—in fact, it can be shown that the reduced EOMs derived through a general, not necessarily quadratic, nonlinear projection, are equivalent to equations (3.8); this is demonstrated in appendix A.

The more general concept of an *invariant manifold* is based on the theory of normal forms, and has been utilised, under its asymptotic formulation, for the reduction of thin shells and beams [25–30,53,55–58]. The invariant manifold approach has the added capacity to allow for coupling

[10]The higher-order nonlinear terms are necessary to accurately capture the effect of the geometric nonlinearity related to the quasi-static coupling between the low-frequency transverse modes and the high-frequency in-plane modes.

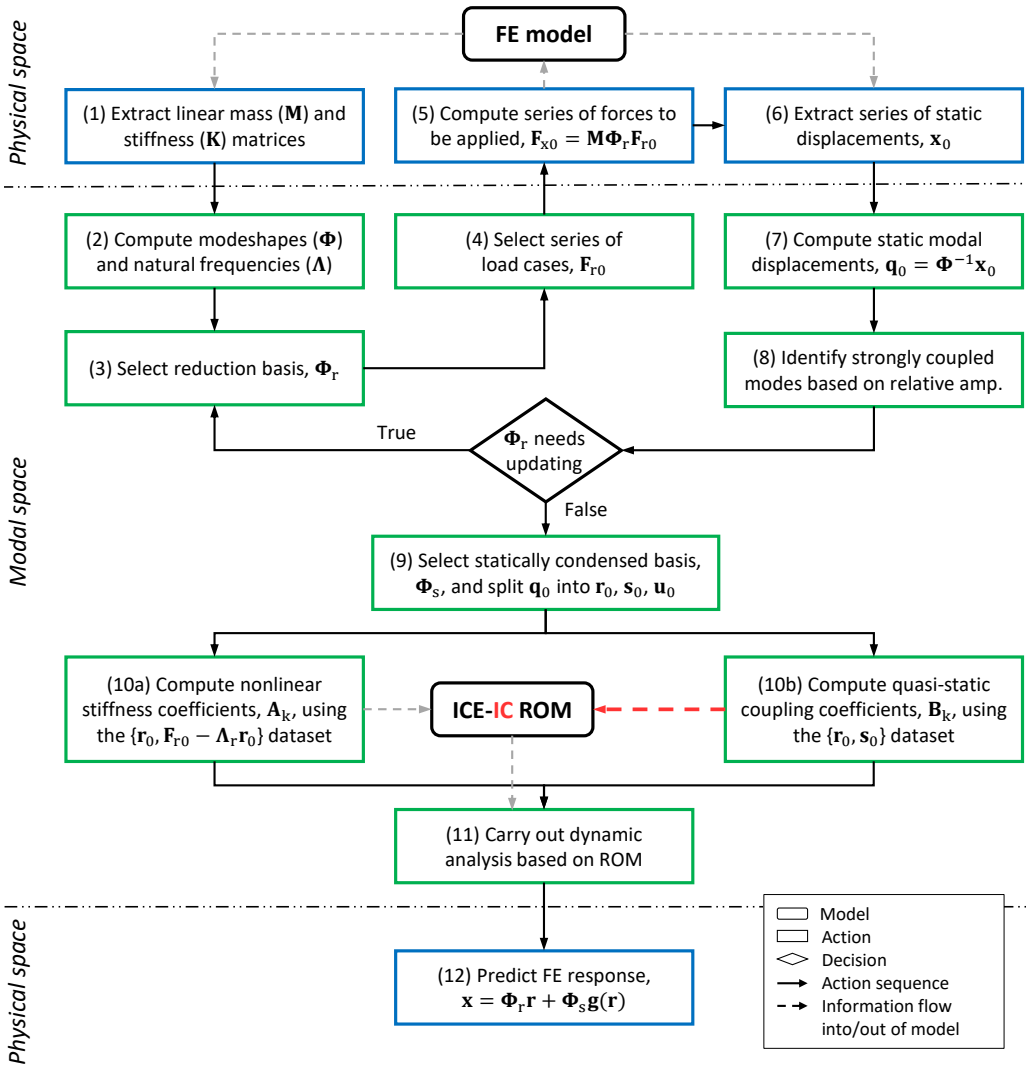

Figure 6: Schematic of the ROM generation procedure using the ICE method, with the schematically modest, but dynamically significant, proposed changes to incorporate inertial compensation shown in red.

between modal displacements and modal velocities, whereas in our proposed method, quasi-static coupling is assumed. However, it has been observed that, for non-gyroscopic, conservative systems, any velocity dependence can be neglected without much loss of accuracy [53,56], making the aforementioned assumption a good approximation. One the other hand, the main limitation of the invariant manifold approach is its high algebraic complexity, which makes the derivation of expressions for manifolds of order higher than cubic, intractable [28]. Even though 3rd-order invariant manifolds can very accurately capture the NNMs of the full-order system at moderate amplitudes, the results deteriorate rapidly beyond a certain amplitude, where higher-order nonlinear terms are necessary to capture the reduced dynamics [28,30,57,58]. With our proposed method, this issue does not occur, since the coefficients of the nonlinear functions in the EOMs are computed *indirectly* via regression analysis, using a set of static solutions of the full-order system. As a result, the expressions that *directly* relate the coefficients of the full-order system to those of the ROM need not be derived, and thus higher orders of nonlinearity can easily be considered.

4. Application to a cantilever beam

We now revisit the FE model of the cantilever beam considered in §2(b) (figure 1(b)). We compare ROMs obtained using the standard ICE method, equation (2.5), with those obtained using the extended ICE-IC method, equation (3.8). The first and second backbone curves of the cantilever beam are considered separately in the following subsections.

(a) First backbone curve

As in §2(b), we consider single-DOF quintic ROMs of the first mode. The standard ICE ROM is described by equation (2.12), whilst the ICE-IC ROM includes some additional terms to account for the kinetic energy of the statically coupled modes, i.e.

$$\left[1+\sum_i\left(\frac{\partial g_i}{\partial r_1}\right)^2\right]\ddot{r}_1+\sum_i\frac{\partial g_i}{\partial r_1}\frac{\partial^2 g_i}{\partial r_1^2}\dot{r}_1^2+\omega_1^2 r_1+A_2r_1^2+A_3r_1^3+A_4r_1^4+A_5r_1^5=F_1, \tag{4.1}$$

where $g_i(r_1)=s_i=B_2^{(i)}r_1^2+B_3^{(i)}r_1^3+B_4^{(i)}r_1^4+B_5^{(i)}r_1^5$ and i spans the indices of the statically coupled LNMs. In this case, only the three most strongly coupled axial modes are included in the statically coupled basis (i.e. $S=3$, $\mathbf{s}\approx\left[q_{27},q_{59},q_{90}\right]^{\mathsf{T}}$). The coefficients in the quasi-static coupling functions, $\mathbf{B}_k$, are computed according to equation (2.9) using the same static solution dataset that is used to compute the nonlinear stiffness coefficients, $\mathbf{A}_k$. As before, this consists of four load cases, where the applied force in the first mode is $F_1=\{-45,-22.5,+22.5,+45\}$. The resulting quasi-static behaviour of the cantilever beam for the range of applied loads is shown in figures 2(b) and 3(b).

Figure 7(a) shows the computed backbone curves of the ICE (blue) and ICE-IC (red) ROMs. It can be seen that the inertial compensation terms have a softening effect on the model, bringing the nonlinear response frequency very close to the underlying linear natural frequency even at large vibration amplitudes—this observation is in agreement with results in the literature [50,58,59]. As in §2(b), we estimate the accuracy of each ROM by computing the free response of the FE model with the initial conditions and period of integration predicted by the ROM. The results obtained from ten different free response runs are shown in figure 7(b,c) for the ICE and ICE-IC ROM, respectively. It can be seen that the novel ROM is able to predict the response frequency of the first NNM of the cantilever beam remarkably well, as it gives rise to nearly perfect free response loops in phase space, for the whole range of amplitudes considered here. It should be noted that, for this system, the computational cost associated with solving the EOMs of the ICE-IC ROM using the MATLAB built-in ode45 solver, is increased by only ~ 4% relative to the ICE ROM.

(b) Second backbone curve

We now consider the second backbone curve of the cantilever beam by computing two-DOF quintic ROMs. As before, the statically coupled basis consists of the 27th, 59th and 90th LNMs, whilst the reduction basis includes both the 1st and 2nd LNMs. The 2-DOF EOMs for the ICE and ICE-IC ROMs are given, respectively, by

$$\begin{bmatrix}\ddot{r}_1\\ \ddot{r}_2\end{bmatrix}+\begin{bmatrix}\omega_1^2 & 0\\ 0 & \omega_2^2\end{bmatrix}\begin{bmatrix}r_1\\ r_2\end{bmatrix}+\begin{bmatrix}\tilde{f}_{r1}(r_1,r_2)\\ \tilde{f}_{r2}(r_1,r_2)\end{bmatrix}=\begin{bmatrix}F_1\\ F_2\end{bmatrix} \tag{4.2}$$

and

$$\begin{aligned}&\begin{bmatrix}\ddot{r}_1\\ \ddot{r}_2\end{bmatrix}+\begin{bmatrix}\omega_1^2 & 0\\ 0 & \omega_2^2\end{bmatrix}\begin{bmatrix}r_1\\ r_2\end{bmatrix}+\begin{bmatrix}\tilde{f}_{r1}(r_1,r_2)\\ \tilde{f}_{r2}(r_1,r_2)\end{bmatrix}\\ &\quad+\sum_i\begin{bmatrix}\left(\frac{\partial g_i}{\partial r_1}\right)^2 & \frac{\partial g_i}{\partial r_1}\frac{\partial g_i}{\partial r_2}\\ \frac{\partial g_i}{\partial r_1}\frac{\partial g_i}{\partial r_2} & \left(\frac{\partial g_i}{\partial r_2}\right)^2\end{bmatrix}\begin{bmatrix}\ddot{r}_1\\ \ddot{r}_2\end{bmatrix}+\sum_i\begin{bmatrix}\frac{\partial g_i}{\partial r_1}\\ \frac{\partial g_i}{\partial r_2}\end{bmatrix}\left(\frac{\partial^2 g_i}{\partial r_1^2}\dot{r}_1^2+2\frac{\partial^2 g_i}{\partial r_1\partial r_2}\dot{r}_1\dot{r}_2+\frac{\partial^2 g_i}{\partial r_2^2}\dot{r}_2^2\right)=\begin{bmatrix}F_1\\ F_2\end{bmatrix},\end{aligned} \tag{4.3}$$

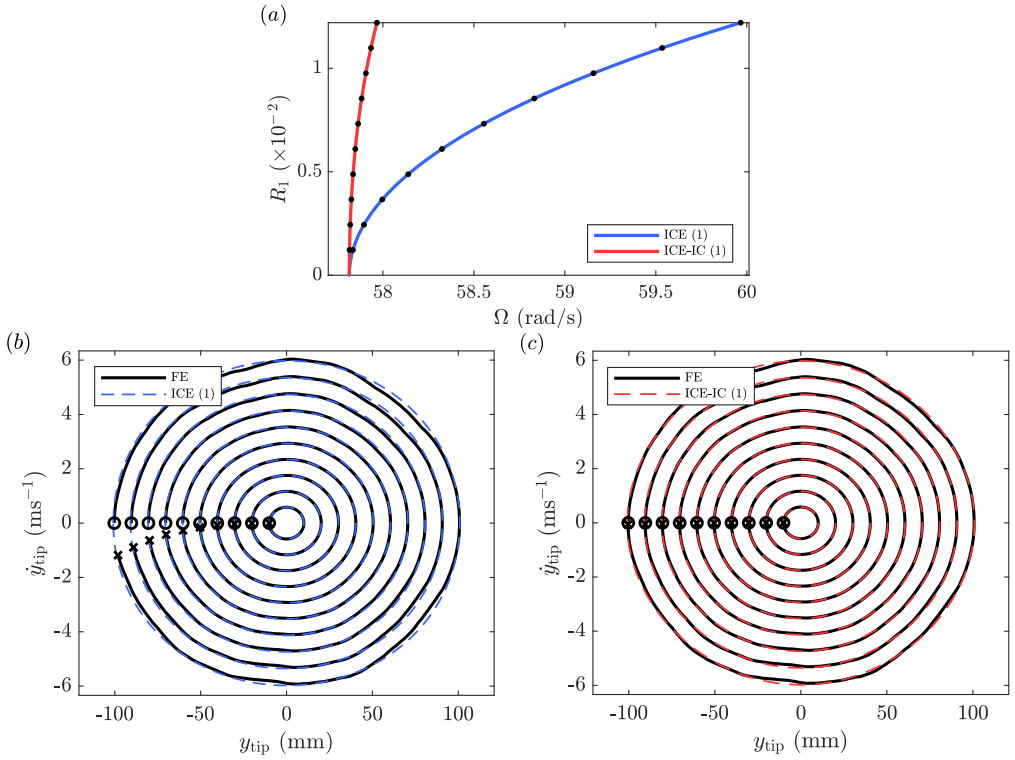

Figure 7: (a) First backbone curve of the C-F beam, predicted by the quintic single-DOF ROMs without (blue) and with (red) inertial compensation. These are plotted in the projection of response frequency against amplitude. Bottom: Comparison between the periodic response predicted by the ROMs (dashed lines) and the response of the FE model (solid black line), plotted in the physical phase space, for (b) the ICE ROM and (c) the ICE-IC ROM. Ten different sets of initial conditions are considered for each ROM, and these are marked with black dots on the backbone curves. For each free response run, the FE states at time $t = 0$ and $t = T_\Omega$ are marked with circles and crosses, respectively.

where $\tilde{f}_{r1}$, $\tilde{f}_{r2}$ and g_i are fifth-order nonlinear polynomial functions of r_1 and r_2.

The coefficients in the nonlinear stiffness functions and in the quasi-static coupling functions were computed using a set of 24 unique static solutions of the FE model. The distribution of the static loads applied in each mode, as well as the corresponding static displacement of the tip node, are shown in figure 8. The magnitude of the maximum load applied in the second mode, $F_2 = 270$, was set to four times that in the first mode, $F_1 = 45$[11]. Table 2 shows the relative displacement amplitudes of the reduced modes (q_1, q_2), as well as the most strongly coupled bending mode (q_3) and axial modes (q_{27}, q_{59}), for four of the considered load cases. It can be seen that, when a force is applied in the second mode, the response of the first mode is significant, which suggests that it must be retained in the reduction basis. As before, the coupling with higher transverse modes is weak, whilst the lowest axial modes are strongly coupled and are thus included in the statically coupled basis.

Figure 9(a,b) shows the backbone curves for the second mode of the computed two-DOF ROMs, shown in the projection of response frequency against the amplitude of each retained mode. It can be seen that, as expected, the traditional ICE ROM fails to capture the softening

[11] Even though the relative scaling of the applied loads was chosen semi-arbitrarily, *a posteriori* computations have confirmed that the ROMs are not greatly dependent on the precise tuning of force scaling factors—as discussed in [47], this is related to the higher orders of nonlinearity considered in the ROMs.

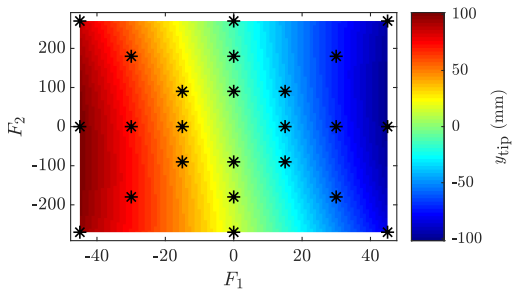

Figure 8: Plot of the vertical displacement of the tip of the C-F beam, as a function of the static forces applied to the first and second modes. The load cases used for calibrating the two-DOF ROMs are marked with black asterisks.

Table 2: Relative modal displacement amplitudes of the most strongly coupled bending and axial modes, for different combinations of static forces applied in the first and second modes.

		Mode no.				
F_1	F_2	1	2	3	27	59
0	270	1.2×10^{-1}	1.0×10^{0}	2.9×10^{-3}	1.5×10^{-1}	5.2×10^{-2}
45	0	1.0×10^{0}	6.3×10^{-3}	3.8×10^{-4}	1.7×10^{-1}	6.7×10^{-2}
45	-270	1.0×10^{0}	1.6×10^{-1}	1.4×10^{-3}	1.7×10^{-1}	2.3×10^{-2}
45	270	1.0×10^{0}	1.7×10^{-1}	5.9×10^{-3}	1.9×10^{-1}	1.2×10^{-1}

behaviour of the second NNM, which arises due to the effect of in-plane inertia. The dominance of the inertial over the geometric nonlinearities in the second backbone curve, as well as in all higher backbone curves of the cantilever beam, is a classical observation in the literature [50–53,58,59]. Figure 9(c,d) shows the phase space plots of ten different free response runs of the FE model, with the initial conditions and period of integration predicted by the ICE and ICE-IC ROMs, respectively. In the case of the ICE ROM, it can be observed that not only is the response frequency overestimated, but the initial conditions predicted by the ROM are such that the full-order response is not periodic, regardless of the period of integration, i.e. the loops gradually shift in phase space. Conversely, the periodic solutions predicted by the ICE-IC ROM satisfy the FE model with excellent accuracy.

5. Conclusion

In this paper, we consider the indirect reduced-order modelling strategy commonly referred to as Implicit Condensation and Expansion, which is applicable to geometrically nonlinear structures modelled using commercial FE software. We have demonstrated its effectiveness, by employing it for the reduction of an FE model of a clamped-clamped beam, as well as its limitations, using a cantilever beam. We have shown that, in the latter example, the large in-plane displacements can give rise to significant amounts of kinetic energy in the high-frequency, statically coupled axial modes. In the ICE method, in-plane kinetic energy is neglected, which leads to results which are quantitatively and qualitatively inaccurate. We have used the concept of an underlying nonlinear manifold to show, using a Lagrangian approach, how the effect of the in-plane kinetic energy can be accounted for in the reduced dynamics. This gives rise to additional terms in the reduced EOMs, relative to the standard ICE ROM, which we term *Inertial Compensation*—the proposed extended method is referred to as ICE-IC. The additional functions in the ICE-IC ROM are formulated using the existing static solution dataset that is used to calibrate the standard ROM.

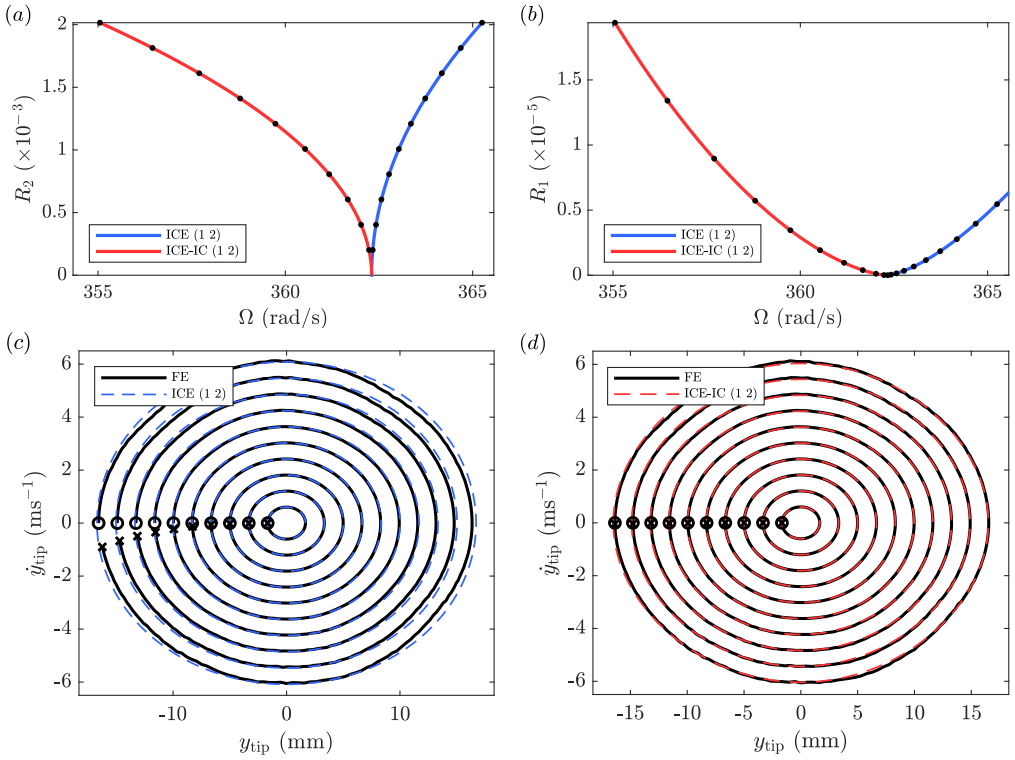

Figure 9: Top: Second backbone curve of the C-F beam, predicted by the quintic two-DOF ROMs without (blue) and with (red) inertial compensation. These are plotted in the projection of response frequency against (a) amplitude of the second mode, and (b) amplitude of the first mode. Bottom: Comparison between the periodic response predicted by the ROMs (dashed lines) and the response of the FE model (solid black line), plotted in the physical phase space, for (c) the ICE ROM and (d) the ICE-IC ROM. Ten different sets of initial conditions are considered for each ROM, and these are marked with black dots on the backbone curves. For each free response run, the FE states at time $t = 0$ and $t = T_\Omega$ are marked with circles and crosses, respectively. The numbers in brackets in the legends denote the modes included in the reduction basis.

Specifically, the additional terms are expressed in terms of the functions which describe the quasi-static coupling between the dynamically important transverse modes and the statically coupled in-plane modes—these are used in the *Expansion* step of the standard ICE method in order to recover the physical displacement of the full-order model, but they are not taken into account when considering the reduced dynamics. We have demonstrated the proposed method using the common engineering example of a cantilever beam example, and shown that excellent accuracy can be obtained. In practical applications, the inertial compensation approach can significantly improve the accuracy and efficiency of ROMs of engineering structures which have similar properties to a cantilever beam, such as wind turbine blades and flexible wings, as well as any other structures where a significant amount of kinetic energy is present in the condensed modes.

Data Accessibility. Data and code submitted as supplementary material.

Authors' Contributions. E.N. led the development of the work, with supervisory support from T.L.H. and S.A.N. on the development of the idea. All authors contributed to the preparation of the manuscript, gave final approval for publication and agree to be held accountable for the work performed therein.

Funding. E.N. is supported by an EPSRC DTP studentship and S.A.N. is supported by an EPSRC Programme grant (EP/R006768/1).

A. Reduction through a nonlinear projection

Here, we demonstrate that the Lagrangian-based approach presented in §3, is equivalent to projecting the EOMs of the full-order system onto an underlying nonlinear manifold. We start by considering the EOMs of the full-order model, split into the reduced, statically coupled, and unmodelled modal coordinates, i.e. equation (2.4). When the response of the third group of modes is neglected, the full-order EOMs can be approximated[12] as

$$\begin{bmatrix}\ddot{\mathbf{r}}\\ \ddot{\mathbf{s}}\end{bmatrix}+\begin{bmatrix}\mathbf{\Lambda}_r & \mathbf{0}\\ \mathbf{0} & \mathbf{\Lambda}_s\end{bmatrix}\begin{bmatrix}\mathbf{r}\\ \mathbf{s}\end{bmatrix}+\begin{bmatrix}\hat{\mathbf{f}}_r(\mathbf{r},\mathbf{s})\\ \hat{\mathbf{f}}_s(\mathbf{r},\mathbf{s})\end{bmatrix}=\begin{bmatrix}\mathbf{F}_r\\ \mathbf{0}\end{bmatrix}. \tag{A.1}$$

Then, since the coordinates in $\mathbf{s}$ are assumed to be statically coupled to the coordinates in $\mathbf{r}$ (equation (2.6)), the system can be reduced using a nonlinear mapping $\boldsymbol{\Gamma}$, defined as

$$\begin{bmatrix}\mathbf{r}\\ \mathbf{s}\end{bmatrix}=\begin{bmatrix}\mathbf{r}\\ \mathbf{g}(\mathbf{r})\end{bmatrix}=\boldsymbol{\Gamma}(\mathbf{r}). \tag{A.2}$$

Differentiating this twice with respect to time, leads to

$$\begin{bmatrix}\dot{\mathbf{r}}\\ \dot{\mathbf{s}}\end{bmatrix}=\frac{\partial\boldsymbol{\Gamma}}{\partial\mathbf{r}}\dot{\mathbf{r}} \tag{A.3a}$$

$$\begin{bmatrix}\ddot{\mathbf{r}}\\ \ddot{\mathbf{s}}\end{bmatrix}=\frac{\partial\boldsymbol{\Gamma}}{\partial\mathbf{r}}\ddot{\mathbf{r}}+\left(\frac{\partial^2\boldsymbol{\Gamma}}{\partial\mathbf{r}^2}\dot{\mathbf{r}}\right)\dot{\mathbf{r}}, \tag{A.3b}$$

where $\dfrac{\partial\boldsymbol{\Gamma}}{\partial\mathbf{r}}$ and $\dfrac{\partial^2\boldsymbol{\Gamma}}{\partial\mathbf{r}^2}$ are, respectively, the Jacobian and vector Laplacian of the nonlinear mapping, with dimensions of $(R+S)\times R$ and $(R+S)\times R\times R$. These can be rewritten as

$$\frac{\partial\boldsymbol{\Gamma}}{\partial\mathbf{r}}=\begin{bmatrix}\mathbf{I}\\ \dfrac{\partial\mathbf{g}}{\partial\mathbf{r}}\end{bmatrix},\quad \frac{\partial^2\boldsymbol{\Gamma}}{\partial\mathbf{r}^2}=\begin{bmatrix}\mathbf{0}\\ \dfrac{\partial^2\mathbf{g}}{\partial\mathbf{r}^2}\end{bmatrix}, \tag{A.4}$$

where $\dfrac{\partial\mathbf{g}}{\partial\mathbf{r}}[i,j]=\dfrac{\partial g_i}{\partial r_j}$, $\dfrac{\partial^2\mathbf{g}}{\partial\mathbf{r}^2}[i,j,k]=\dfrac{\partial^2 g_i}{\partial r_j\partial r_k}$, $\mathbf{I}$ is the $R\times R$ identity matrix and $\mathbf{0}$ is the $R\times R\times R$ zero tensor. Substituting equations (A.2) and (A.3) into equation (A.1) and premultiplying by the transpose of the tangent subspace [22,23], $\left(\dfrac{\partial\boldsymbol{\Gamma}}{\partial\mathbf{r}}\right)^{\mathsf{T}}$, leads to

$$\left(\frac{\partial\boldsymbol{\Gamma}}{\partial\mathbf{r}}\right)^{\mathsf{T}}\left[\frac{\partial\boldsymbol{\Gamma}}{\partial\mathbf{r}}\ddot{\mathbf{r}}+\left(\frac{\partial^2\boldsymbol{\Gamma}}{\partial\mathbf{r}^2}\dot{\mathbf{r}}\right)\dot{\mathbf{r}}\right]+\left(\frac{\partial\boldsymbol{\Gamma}}{\partial\mathbf{r}}\right)^{\mathsf{T}}\begin{bmatrix}\mathbf{\Lambda}_r & \mathbf{0}\\ \mathbf{0} & \mathbf{\Lambda}_s\end{bmatrix}\boldsymbol{\Gamma}+\left(\frac{\partial\boldsymbol{\Gamma}}{\partial\mathbf{r}}\right)^{\mathsf{T}}\begin{bmatrix}\hat{\mathbf{f}}_r(\mathbf{r},\mathbf{g})\\ \hat{\mathbf{f}}_s(\mathbf{r},\mathbf{g})\end{bmatrix}=\left(\frac{\partial\boldsymbol{\Gamma}}{\partial\mathbf{r}}\right)^{\mathsf{T}}\begin{bmatrix}\mathbf{F}_r\\ \mathbf{0}\end{bmatrix}. \tag{A.5}$$

Finally, after substituting equations (A.4) into equation (A.5), and some algebraic manipulation, equation (3.8) is obtained.

References

1. Reddy JN. 1993 *An introduction to the finite element method*. New York: McGraw-Hill.
2. Nayfeh AH, Mook DT. 1979 *Nonlinear Oscillations*. New York: Wiley-Interscience.
3. Nayfeh AH. 1981 *Introduction to Perturbation Techniques*. New York: Wiley-Interscience.
4. Jezequel L, Lamarque CH. 1991 Analysis of non-linear dynamical systems by the normal form theory. *Journal of sound and vibration* **149**, 429–459.
5. Dankowicz H, Schilder F. 2013 *Recipes for continuation* vol. 11. Philadelphia, PA: SIAM.
6. Doedel EJ, Champneys AR, Fairgrieve TF, Kuznetsov YA, Oldeman BE, Paffenorth RC, Sandstede B, Wang X, Zhang C. 2007 AUTO-07P: Continuation and bifurcation software for ordinary differential equations. .
7. Crisfield MA. 1993 *Non-linear finite element analysis of solids and structures* vol. 1. Wiley New York.

[12] Note that this is equivalent to applying the Euler-Lagrange equation to the approximated Lagrangian, equation (3.3).

8. Nash M. 1977 *Nonlinear Structural Dynamics by Finite Element Modal Synthesis*. PhD thesis Imperial College, University of London.
9. Mei C, Moorthy J. 1995 Numerical simulation of the nonlinear response of composite plates under combined thermal and acoustic loading. .
10. Shi Y, Mei C. 1996 A finite element time domain modal formulation for large amplitude free vibrations of beams and plates. *Journal of Sound and Vibration* **193**, 453–464.
11. Przekop A, Azzouz MS, Guo X, Mei C, Azrar L. 2004a Finite element multiple-mode approach to nonlinear free vibrations of shallow shells. *AIAA journal* **42**, 2373–2381.
12. Przekop A, Guo X, Azzouz S, Mei C. 2004b Reinvestigation of nonlinear random response of shallow shells using finite element modal formulation. In *45th AIAA/ASME/ASCE/AHS/ASC Structures, Structural Dynamics & Materials Conference* p. 1553.
13. Jacob B, Ebecken N. 1992 Adaptive reduced integration method for nonlinear structural dynamic analysis. *Computers & structures* **45**, 333–347.
14. Idelsohn SR, Cardona A. 1985a A reduction method for nonlinear structural dynamic analysis. *Computer Methods in Applied Mechanics and Engineering* **49**, 253–279.
15. Idelsohn SR, Cardona A. 1985b A load-dependent basis for reduced nonlinear structural dynamics. *Computers & Structures* **20**, 203–210.
16. Slaats P, De Jongh J, Sauren A. 1995 Model reduction tools for nonlinear structural dynamics. *Computers & structures* **54**, 1155–1171.
17. Rutzmoser JB. 2018 *Model Order Reduction for Nonlinear Structural Dynamics*. PhD thesis Technische Universität München.
18. Tiso P, Jansen E, Abdalla M. 2011 Reduction method for finite element nonlinear dynamic analysis of shells. *AIAA journal* **49**, 2295–2304.
19. Wu L, Tiso P. 2016 Nonlinear model order reduction for flexible multibody dynamics: a modal derivatives approach. *Multibody System Dynamics* **36**, 405–425.
20. Sombroek CS, Tiso P, Renson L, Kerschen G. 2018 Numerical computation of nonlinear normal modes in a modal derivative subspace. *Computers & Structures* **195**, 34–46.
21. Tiso P. 2011 Optimal second order reduction basis selection for nonlinear transient analysis. In *Modal Analysis Topics, Volume 3* pp. 27–39. Springer.
22. Jain S, Tiso P, Rutzmoser JB, Rixen DJ. 2017 A quadratic manifold for model order reduction of nonlinear structural dynamics. *Computers & Structures* **188**, 80–94.
23. Rutzmoser JB, Rixen DJ, Tiso P, Jain S. 2017 Generalization of quadratic manifolds for reduced order modeling of nonlinear structural dynamics. *Computers & Structures* **192**, 196–209.
24. Shaw SW, Pierre C. 1991 Non-linear normal modes and invariant manifolds. *Journal of Sound and Vibration* **150**, 170–173.
25. Shaw SW, Pierre C. 1993 Normal modes for non-linear vibratory systems. *Journal of Sound and Vibration* **164**, 85–124.
26. Shaw SW, Pierre C. 1994 Normal modes of vibration for non-linear continuous systems. *Journal of Sound and Vibration* **169**, 319–347.
27. Pesheck E. 2000 *Reduced order modeling of nonlinear structural systems using nonlinear normal modes and invariant manifolds*. PhD thesis The University of Michigan.
28. Touzé C, Thomas O, Huberdeau A. 2004 Asymptotic non-linear normal modes for large-amplitude vibrations of continuous structures. *Computers & structures* **82**, 2671–2682.
29. Touzé C, Amabili M, Thomas O. 2008 Reduced-order models for large-amplitude vibrations of shells including in-plane inertia. *Computer methods in applied mechanics and engineering* **197**, 2030–2045.
30. Touzé C, Amabili M. 2006 Nonlinear normal modes for damped geometrically nonlinear systems: Application to reduced-order modelling of harmonically forced structures. *Journal of sound and vibration* **298**, 958–981.
31. Mignolet MP, Przekop A, Rizzi SA, Spottswood SM. 2013 A review of indirect/non-intrusive reduced order modeling of nonlinear geometric structures. *Journal of Sound and Vibration* **332**, 2437–2460.
32. Muravyov AA, Rizzi SA. 2003 Determination of nonlinear stiffness with application to random vibration of geometrically nonlinear structures. *Computers & Structures* **81**, 1513–1523.
33. Gordon R, Hollkamp J. 2011 Reduced-order models for acoustic response prediction. Technical Report AFRL-RB-WP-TR-2011-3040 Air Force Research Laboratory Dayton, OH.
34. Rizzi SA, Przekop A. 2005 The effect of basis selection on static and random acoustic response prediction using a nonlinear modal simulation. .

35. Tartaruga I, Elliott A, Hill TL, Neild SA, Cammarano A. 2019 The effect of nonlinear cross-coupling on reduced-order modelling. *International Journal of Non-Linear Mechanics* **116**, 7–17.
36. Rizzi SA, Przekop A. 2008 System identification-guided basis selection for reduced-order nonlinear response analysis. *Journal of Sound and Vibration* **315**, 467–485.
37. Kuether RJ, Deaner BJ, Hollkamp JJ, Allen MS. 2015 Evaluation of geometrically nonlinear reduced-order models with nonlinear normal modes. *AIAA Journal* **53**, 3273–3285.
38. Wang X, Mignolet M, Eason T, Spottswood S. 2009 Nonlinear reduced order modeling of curved beams: a comparison of methods. In *50th AIAA/ASME/ASCE/AHS/ASC Structures, Structural Dynamics, and Materials Conference* p. 2433.
39. Kim K, Radu AG, Wang X, Mignolet MP. 2013 Nonlinear reduced order modeling of isotropic and functionally graded plates. *International Journal of Non-Linear Mechanics* **49**, 100–110.
40. Hollkamp J, Gordon R, Spottswood S. 2003 Nonlinear sonic fatigue response prediction from finite element modal models: a comparison with experiments. In *44th AIAA/ASME/ASCE/AHS/ASC Structures, Structural Dynamics, and Materials Conference* p. 1709.
41. Hollkamp JJ, Gordon RW, Spottswood SM. 2005 Nonlinear modal models for sonic fatigue response prediction: a comparison of methods. *Journal of Sound and Vibration* **284**, 1145–1163.
42. Przekop A, Rizzi SA. 2006 A reduced order method for predicting high cycle fatigue of nonlinear structures. *Computers & structures* **84**, 1606–1618.
43. Segalman D, Dohrmann C. 1996 A method for calculating the dynamics of rotating flexible structures, part 1: Derivation. *Journal of Vibration and Acoustics* **118**, 313–317.
44. Segalman D, Dohrmann C, Slavin A. 1996 A method for calculating the dynamics of rotating flexible structures, part 2: Example calculations. *Journal of Vibration and Acoustics* **118**, 318–322.
45. McEwan M, Wright JR, Cooper JE, Leung AYT. 2001 A combined modal/finite element analysis technique for the dynamic response of a non-linear beam to harmonic excitation. *Journal of Sound and Vibration* **243**, 601–624.
46. Hollkamp JJ, Gordon RW. 2008 Reduced-order models for nonlinear response prediction: Implicit condensation and expansion. *Journal of Sound and Vibration* **318**, 1139–1153.
47. Nicolaidou E, Melanthuru VR, Hill TL, Neild SA. 2020 Accounting for Quasi-Static Coupling in Nonlinear Dynamic Reduced-Order Models. *Journal of Computational and Nonlinear Dynamics* **15**.
48. Papazafeiropoulos G, Muñiz-Calvente M, Martínez-Pañeda E. 2017 Abaqus2Matlab: a suitable tool for finite element post-processing. *Advances in Engineering Software* **105**, 9–16.
49. Kuether RJ, Allen MS. 2014 A numerical approach to directly compute nonlinear normal modes of geometrically nonlinear finite element models. *Mechanical Systems and Signal Processing* **46**, 1–15.
50. Haight E, King W. 1972 Stability of nonlinear oscillations of an elastic rod. *The Journal of the Acoustical Society of America* **52**, 899–911.
51. Pai PF, Nayfeh AH. 1990 Non-linear non-planar oscillations of a cantilever beam under lateral base excitations. *International Journal of Non-Linear Mechanics* **25**, 455–474.
52. Nayfeh AH, Chin C, Nayfeh SA. 1995 Nonlinear Normal Modes of a Cantilever Beam. *Journal of Vibration and Acoustics* **117**, 477–481.
53. Hsieh SR, Shaw SW, Pierre C. 1994 Normal modes for large amplitude vibration of a cantilever beam. *International Journal of Solids and Structures* **31**, 1981–2014.
54. Rutzmoser JB, Rixen DJ, Tiso P. 2014 Model order reduction using an adaptive basis for geometrically nonlinear structural dynamics. In *International Conference on Noise and Vibration Engineering, ISMA, Leuven, Belgium*.
55. Pesheck E, Boivin N, Pierre C, Shaw SW. 2001 Nonlinear modal analysis of structural systems using multi-mode invariant manifolds. *Nonlinear Dynamics* **25**, 183–205.
56. Shaw SW, Pierre C, Pesheck E. 1999 Modal Analysis-Based Reduced-Order Models for Nonlinear Structures – An Invariant Manifold Approach. *The Shock and Vibration Digest* **31**, 3–16.
57. Touzé C, Thomas O, Chaigne A. 2004 Hardening/softening behaviour in non-linear oscillations of structural systems using non-linear normal modes. *Journal of Sound and Vibration* **273**, 77–101.
58. Touzé C, Thomas O. 2004 Reduced-order modeling for a cantilever beam subjected to harmonic forcing. In *Proceedings of the EUROMECH Colloquium 457: Non-linear Modes of Vibrating Systems*, pp. 165–168.
59. Pai PF. 2007 *Highly flexible structures: modeling, computation, and experimentation*. American Institute of Aeronautics and Astronautics.